Contents lists available at ScienceDirect

Separation and Purification Technology

journal homepage: www.elsevier.com

Highly effective asphaltene-derived adsorbents for gas phase removal of volatile organic compounds

Maksymilian Plata-Gryl [a], Malwina Momotko [a], Sławomir Makowiec [b], Grzegorz Boczkaj [a], *

[a] *Gdansk University of Technology, Faculty of Chemistry, Department of Process Engineering and Chemical Technology, Poland*
[b] *Gdansk University of Technology, Faculty of Chemistry, Department of Organic Chemistry, Poland*

ARTICLE INFO

Keywords:
Asphaltenes
Adsorption
VOC
Waste gases
Treatment
Adsorption isotherms

ABSTRACT

A novel nitrated asphaltene-derived adsorbent (Asf-Nitro) was prepared using facile isolation and modification procedures. The successful modification was confirmed by Fourier-transform infrared spectroscopy (FTIR). The nitrated adsorbent was evaluated in terms of dispersive and specific interactions, Lewis acid-base properties and adsorption isotherms by means of inverse gas chromatography (IGC). Nitration was found to be extremely effective in enhancing adsorption properties of asphaltenes towards variety of chemical compounds. Asf-Nitro adsorbent exhibits superior dispersive interactions ($197.50 \pm 1.12\,\mathrm{mJ\,m^{-2}}$ at 423 K), as compared to unmodified asphaltenes, which are comparable with activated carbons, zeolites or alumina. Examination of the specific interactions revealed a shift from basic to acidic character of the surface, what will be beneficial for adsorption of alkaline gases. Additionally, adsorption isotherms revealed that developed surface properties of the Asf-Nitro results in more than doubled monolayer adsorption capacity. Obtained results demonstrates the applicability of the asphaltene-derived materials in adsorption processes as highly effective and low cost adsorbents. This studies revealed a highly effective adsorption of environmentally important VOCs, e.g. *n*-butanol (odorous compound), trichloromethane (chlorinated hydrocarbon) and benzene (carcinogenic).

1. Introduction

Volatile organic compounds (VOCs) are a large group of organic chemical compounds having vapor pressure of at least 0.01 kPa at standard conditions [1]. They are present as gaseous airborne chemicals and as chemicals adsorbed on solids (indoor surfaces, airborne particular matter) [2,3]. The effects of some groups of VOCs on human health as well as ecosystems [4] relate to number of acute or chronic hazards e.g.: cancer, allergies, respiratory and immune effects, central nervous systems dysfunctions, formation of tropospheric ozone and photochemical smog [5–7].

Apart from increased health risk and ecosystems deterioration, VOCs can be problematic even if their toxicity is not confirmed. Odorous compounds emitted from industries and landfills can decrease the quality of life and pose a problem for a company's image, since odors are commonly perceived as an indicator of harmful and toxic activity [8,9]. This issue is gaining particular importance due to development of both industrial and residential areas [10,11].

The issue of VOCs emission from anthropogenic sources is acknowledged and demand for VOCs emission control is increasing an enforcement of environmental legislations, e.g. European Union obliged member states to cut the emission of VOCs by 40% till 2030 [12]. Development of separation techniques is a part of remedial measures to reduce emission of VOCs.

Among the available technologies for removal of VOCs, adsorption-based processes proved their usefulness and effectiveness in purification and separation of gaseous streams [13,14]. Since the key parameter in adsorption processes is a type of adsorbent, the main developments in this field are focused on new adsorbents [15]. To replace commonly used activated carbon, zeolites, silica or polymers, new adsorbent must exhibit unique adsorption properties or/and its application must be economically feasible. Three main trends in the research on new adsorbents can be observed:

---

* Corresponding author at: Gdansk University of Technology, Faculty of Chemistry, Department of Process Engineering and Chemical Technology, G. Narutowicza St. 11/12, 80-233 Gdansk, Poland.
Email address: grzegorz.boczkaj@pg.edu.pl (G. Boczkaj)

https://doi.org/10.1016/j.seppur.2019.05.041
Received 29 January 2019; Received in revised form 8 May 2019; Accepted 9 May 2019
Available online xxx

Post-print of: Plata-Gryl M., Momotko M., Makowiec S., Boczkaj G.: Highly effective asphaltene-derived adsorbents for gas phase removal of volatile organic compounds. SEPARATION AND PURIFICATION TECHNOLOGY. Vol. 224 (2019), pp. 315-321. DOI: https://doi.org/10.1016/j.seppur.2019.05.041

(1) synthesis of new types of adsorbents e.g. carbon nanotubes, graphene [16], molecular organic frameworks [17],
(2) development of low-cost activated carbon prepared from waste materials [18–20]
(3) direct application of natural materials as bio-adsorbents [21,22]

An interesting alternative for traditional sorbents can be asphaltenes. They are carbonaceous material with high C:H ratio of about 1–1.2 and the most aromatic fraction of the crude oil and the heaviest products of its processing, quantitatively remaining in residue from vacuum distillation. Asphaltenes are numerous group of polycyclic aromatic hydrocarbons (PACs) defined on the basis of solubility - as a fraction insoluble in *n*-alkanes and soluble in toluene or benzene. They are comprised of 4–10 fused aromatic rings, peripherally attached alkyl chains and polar functional groups, with tendency to stacking and formation of graphite-like structure. Besides carbon and hydrogen, heteroatoms such as oxygen, sulfur, nitrogen and trace amount of metals can be found in their backbone [23–28].

Asphaltenes structure i.e. aromatic ring, alkyl chains, polar functional groups (carboxylic, phenol, pyridine) is a source of a vast variety of interactions e.g. van der Waals, coulombic, hydrogen bonding and π-π stacking [29].

In petroleum industry uncontrolled asphaltene precipitation is a source of severe technological issues during crude oil processing eg. well-bore and pipeline clogging, catalyst deactivation, fouling, coke and emulsion formation [30,31]. The only practical application of asphaltenes is production of bitumen and bitumen mixtures. In petroleum industry there is significant interest in separating asphaltene fraction from process streams. Due to this reasons, asphaltenes can be treated as a undesired by product or waste.

Recently it was shown that asphaltenes can be applied as sorbents in separation techniques, due to their unique selectivity and thermal stability [32] and simplified isolation procedure of asphaltenes using residue from vacuum distillation of crude oil was proposed [33]. Their application as sorbents would lead to valorization of the by-product, reduction of the costs and would enhance company's competitiveness.

Modification of the surface chemistry can be a feasible direction toward novel applications [34]. Surface modifications that can improve or extend adsorption properties of adsorbents are widely investigated [34–39]. Heteroatoms present on a surface of an adsorbent affects the adsorption capacity and selectivity. In the literature studies on the sulfonation [39], amination [38], methylation [37], nitration [36], ammonia [35] or ozone treatment effects on the adsorption properties can be found. The diverse structure of asphaltene molecules make them especially prone to chemical modifications, thus opening many routes toward tuning their properties for particular adsorption applications [34].

The objective of this study was to evaluate the possibility of utilizing asphaltene fraction in adsorption-based processes. To enhance the surface and adsorption properties of the asphaltene fraction, its properties were tuned by a chemical modification. To evaluate the effect of the chemical modification on the performance of the asphaltene-based sorbents in adsorption processes, inverse gas chromatography (IGC) technique was used. It is a variant of gas chromatography in which a material to be investigated is placed inside a column and characterized by monitoring of the retention of probe molecules with known properties under dynamic conditions. IGC measurements can be carried out at infinite dilution and finite concentration. At infinite dilution adsorbate-adsorbent interactions are the leading cause of adsorption effects and the retention data can be converted into e.g. dispersive and specific components of the free energy of adsorption. At finite concentration, for example, adsorption isotherms can be obtained. Among test probes were environmentally important VOCs, e.g. *n*-butanol (odorous compound), trichloromethane (chlorinated hydrocarbon) and benzene (carcinogenic).

2. Experimental

Informations about the origin of bitumen samples and the asphaltene isolation method and purity control procedure can be found in Text S1.

2.1. Chemical modification (nitration) of the asphaltene fraction

Nitrated asphaltenes were modified as follows: HNO_3 (65%, 6.4 cm^3, 91 mmol) was added to a stirred solution of asphaltene (1.59 g) in CH_2Cl_2 (50 ml). The mixture was refluxed and stirred for 16 h. After this time, solvent was removed under reduced pressure (ca. 10 mmHg). Residue was suspended in methanol (50 ml) and filtered off. The precipitate was washed with methanol (20 ml) and dried under vacuum at 80 °C for 8 h. Successful modification was confirmed by the Fourier-transform infrared spectroscopy (FTIR). Details of the FTIR analysis procedure are described in Text S2.

2.2. Adsorbent preparation

Asphaltene-derived adsorbents (raw asphaltenes – Asf and nitrated asphaltenes – Asf-Nitro) were prepared by coating the Chromosorb W AW DMCS 80/100 mesh (Johns-Manville, USA) with asphaltenes (adsorbent). Chromosorb W (further denoted as Ch-W) is a hydrophobic support with large irregular pores and has BET surface area of 0.6–1.3 $m^2 g^{-1}$. Textural properties (i.e. low surface area values, absence of micropores) of the support ensures that only surface's characteristic influences the adsorption experiments. Moreover it eliminates issues with diffusion into pores and on a surface of an adsorbent.

Detailed description of the coating procedure can be found in [32]. The content of the adsorbent on the support was 10% by mass. It is worth to mention that during the immobilization of asphaltenes on the Ch-W a total coverage is obtained, thus support characteristics in terms of molecular interactions with solutes is negligible.

2.3. Inverse gas chromatography measurements

IGC measurements were carried out using Clarus 500 gas chromatograph equipped with flame ionization detector (Perkin Elmer, USA). Preliminary studies revealed that sorption properties of asphaltenes strongly depend on the temperature and that there is nonlinear change in asphaltene's surface properties at about 453 K. To observe that change in detail, measurements were carried out in the 423–473 K temperature range with 5 K increments. Since retention on Ch-W was insufficient at that temperatures, it was lowered to the 313–333 K range with 5 K increments. Temperature of both the injection port and the detector were 573 K. The carrier gas was nitrogen (N5.0, Linde Gas, Poland) and a flow rate of 20 ml min^{-1} was used. The FID detector was supplied by N5.5 hydrogen from the PGXH2 500 generator (Perkin Elmer, USA) and air from the GC 3000 zero air generator (Perkin Elmer, USA).

To perform IGC experiments at infinite dilution (near zero surface coverage), when adsorption is described by Henry's law, repeatedly smaller samples of vapors from the headspace of the probe compounds were injected by a gas-tight syringe into the GC injector operated in splitless mode. Each probe was injected separately. Retention time was calculated from the peak maximum when there was no change in retention time for three consequent injections. To determine dead (void) time, methane was used as a non-interacting, with a stationary phase, compound at conditions used in this study. Test probes used in IGC experiments are listed in Table S1. *n*-Alkanes were used as standard compounds to evaluate dispersive interactions. Selected polar test probes represents various chemical groups of compounds with different chemical and physical properties. It allows to precisely characterize surface's adsorption properties.

Main parameter calculated in IGC experiments is the net retention volume [40] or specific retention volume (per gram of adsorbent) [41–43]. Here it was calculated according to Eq. (1):

$$\mathrm{V_N} = \frac{\mathrm{j}}{\mathrm{m}}\mathrm{F}(\mathrm{t_R} - \mathrm{t_0}) \tag{1}$$

where t_R (min) is the retention time of given probe, t_0 (min) is the void time measured with a non–interacting probe (methane), F ($\mathrm{mL\,min^{-1}}$) is the flow rate measured at the temperature of experiment, j (–) is the James-Martin correction factor taking into account the compressibility of the gas [44] and m (g) is the mas of the adsorbent coated onto support.

Based on V_N value, the molar free energy of adsorption ΔG_A ($\mathrm{J\,mol^{-1}}$) can be calculated by Eq. (2):

$$\Delta\mathrm{G_A} = -\mathrm{RTlnV_N} + \mathrm{C} \tag{2}$$

where R ($\mathrm{J\,K^{-1}\,mol^{-1}}$) is the gas constant, T (K) is the absolute temperature and C is a constant.

The differential heat of adsorption ΔH_A ($\mathrm{J\,mol^{-1}}$) and the standard entropy of adsorption ΔS_A ($\mathrm{J\,mol^{-1}}$) can be derived from the well-known van't Hoff equation.

The free surface energy of a solid is a sum of dispersive (γ_S^D) and specific components (γ_S^{SP}). For non-polar probes, such as alkanes, only dispersive interactions occurs with the surface of the solid. Hence, the value of γ_S^D can be obtained from the ΔG_A values calculated for the series of *n*-alkanes [45]. To obtain the value of the γ_S^D, the Dorris-Gray method was used [46] in which it is calculated from Eq. (3). Fig. S1 summarize the method of γ_S^D determination.

$$\gamma_\mathrm{S}^\mathrm{D} = \frac{\left(-\Delta\mathrm{G_{CH2}}\right)^2}{4\mathrm{N}^2(\mathrm{a_{CH2}})^2\gamma_\mathrm{CH2}} \tag{3}$$

where N is the Avogadro's number ($\mathrm{mol^{-1}}$), ΔG_{CH_2} ($\mathrm{J\,mol^{-1}}$) is the free energy of adsorption per methylene group. It can be obtained from the slope of the ΔG_A versus the number of carbon atoms in the *n*-alkane molecule. a_{CH_2} ($\mathrm{m^2}$) is the surface area of methylene group. In this work the most common value of 6 $\mathrm{\AA^2}$ was used, although other values can be found in the literature [45]. γ_{CH_2} ($\mathrm{J\,mol^{-1}}$) is the surface energy of the polyethylene-type polymer with finite molecular weight and is calculated according to Eq. (4) [45]:

$$\gamma_\mathrm{CH2} = (35.6 + 0.058\,(293 - \mathrm{T}))\cdot 10^{-3} \tag{4}$$

By injecting polar probes into the column, specific interactions between polar probes and an adsorbent can be observed. Extent of that interactions can be measured with different methods [45] all based on the same assumption that:

$$\Delta\mathrm{G_A} = \Delta\mathrm{G_A^d} + \Delta\mathrm{G_A^{sp}} \tag{5}$$

where ΔG_A^{SP} ($\mathrm{J\,mol^{-1}}$) refers to specific interactions (the specific free energy of adsorption) of a polar molecule adsorbed on a solid.

Specific free energies of adsorption were calculated using Papirer's method [47,48]. Plotting values of ΔG_A for series of *n*-alkanes against the logarithm of the vapor pressure (P^0) of the probe at the experimental temperature, will result in a straight line. ΔG_A^{SP} can be calculated as a difference between ΔG_A obtained for the polar probe and ΔG_A of a hypothetical alkane with the same vapor pressure. The principle of the measurement is presented in Fig. S2. The advantage of the Papirer's method are easily accessible P^0 values for test probes in wide temperature ranges.

Knowing the extent of the specific interactions, the acidic (electronacceptor) and basic (electrondonor) properties of a solid can be determined. Calculations of specific interactions revealed nonlinear dependence of $\Delta G_A^{SP}/T$ versus $1/T$ ($R^2 = 0.7$–0.95), thus ΔH_A^{SP} could not be determined, at least without enormous uncertainty. It prevent usage of donor (DN) and acceptor (AN) numbers that are commonly used to assess acidic and basic properties of a solid, when specific interactions varies linearly with temperature. Instead, Good and van Oss equation [49] was used to obtain the acidic (γ_S^+) and basic (γ_S^-) parameters of the asphaltene adsorbents. Based on the values of aforementioned parameters, the specific component of the surface free energy can be determined (γ_S^{SP}). Details of the calculation procedure are presented in Text S3.

Adsorption isotherms were determined according to the peak maximum method at finite concentration as described elsewhere [50,51]. Adsorption isotherms were measured at three temperatures i.e. 423, 448 and 473 K for selected noxious VOCs i.e. TCM (chlorinated hydrocarbon), benzene (carcinogenic) and *n*-butanol (odorous). The isotherm calculation method is described in more depth in Text S4 and in Fig. S3.

Experimental data were fitted by non-linear regression to BET isotherm model. Computations were performed in R [52] using minipack.ln package which utilizes Levenberg-Marquardt nonlinear least-squares algorithm [53]. Based on the maximum monolayer adsorption capacity, surface areas occupied by the adsorbate were calculated. Details are provided in Text S5.

2.4. Quality assurance of data

All data points obtained by GC measurements and presented in this paper are an average of three injections. The values reported in the following section are given with 95% confidence interval.

3. Results and discussion

Fig. 1 presents infrared absorption spectra of raw (Asf) and modified (Asf-Nitro) asphaltenes. FTIR-ATR spectroscopy was used to determine functional group types in tested samples. FTIR spectra of both samples revealed intensive bands near 2920, 2850 and 1455 $\mathrm{cm^{-1}}$ because of the CH_2 and CH_3 groups. For that groups peak at 1375 $\mathrm{cm^{-1}}$ is also characteristic [54]. It is clearly visible in the spectrum for Asf, while on Asf-Nitro spectrum it is overlaid by stronger absorption band at 1337 $\mathrm{cm^{-1}}$. Bands at 2920, 2850, 1450 and 1375 $\mathrm{cm^{-1}}$ corresponds to vibrations of the methyl group in aliphatic chains. Interestingly, no absorption above 3100 $\mathrm{cm^{-1}}$ was observed, indicating lack of OH groups. Small band visible in both spectra, at around 700 $\mathrm{cm^{-1}}$ can be related to alkyl chains longer than 4 methylene units [55]. The absorbance bands observed between 730 and 870 $\mathrm{cm^{-1}}$ can be assigned to the aromatic C—H out-of-plane bending vibrations [56]. Cleary visible band close to 1030 $\mathrm{cm^{-1}}$ can be related to sulfoxide functional group [57] or to ester linkages [58]. Absorption bands at 1262 (Asf) and 1274 (Asf-Nitro) $\mathrm{cm^{-1}}$ can be attributed to groups containing singly bonded oxygen eg. esters or ethers [59]. Distinct band observed at the 1600 $\mathrm{cm^{-1}}$ in the Asf spectrum is related to the aromatic C═C stretching vibration [55]. In the Asf-Nitro spectrum that band is overlaid by the strong absorption at 1337 $\mathrm{cm^{-1}}$. Three new intensive bands, that can be observed in the Asf-Nitro spectrum, at 1529, 1337 and 1272 $\mathrm{cm^{-1}}$ are a clear confirmation of successful nitration of the asphaltenes, as they can be related to the asymmetrical and symmetrical

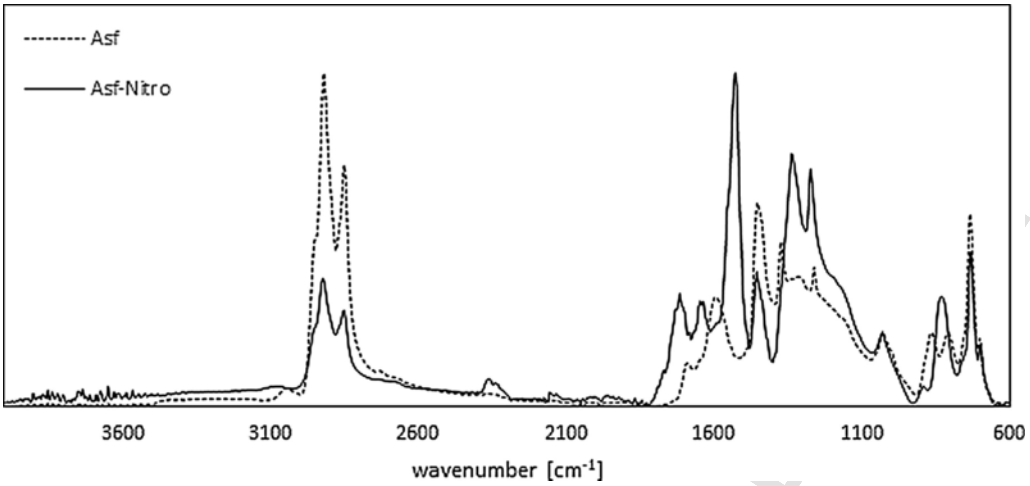

Fig. 1. Normalized FTIR spectra of the asphaltene samples.

aromatic C-NO_2 and N═O stretching, respectively [60]. Additional new peak in the Asf-Nitro spectrum at 1715 cm^{-1} corresponds to the carbonyl functionality [61], what may be a result of the oxidation and together with the increased absorption at 1274 cm^{-1} indicates increased presence of ester functionalities.

Quantitative assessment of the structural features and the effect of the chemical modification on the structure of asphaltenes can be determined based on an approach that can be found e.g. in [62,63]. It is based on the absorption intensity ratios of characteristic bands and the results are presented in Text S6 and Table S2.

Table 1 presents values of the enthalpy and entropy of adsorption of test probes on the investigated materials. Obtained values of enthalpies confirmed that the process is exothermic and negative values of ΔS_A implies that the degree of freedom decreased at the gas-solid interface, what is expected in adsorption process. Compared to ΔH_{liq} (see Table S1), ΔH_A have much lower values (higher absolute values) on Asf and Asf-Nitro, which indicate that measured enthalpies of adsorption are not only due to condensation but also due to physic-chemical interactions between adsorbate and adsorbent. As a result of nitration the value of enthalpy of adsorption increased about one and a half times compared to unmodified asphaltenes. The biggest change was observed for *n*-butanol (1.81 times higher) and the smallest for TCM (1.30 times higher). Similar change in the value of ΔH_A for both the alkanes and polar probes indicates that the most significant difference is in dispersion forces, since alkanes are not capable of specific interaction. The change in the value of entropies followed the same trend as in case of enthalpies.

For Chromosorb W adsorption experiments at temperatures suitable for asphaltene sorbents were infeasible, thus measurements were conducted at 40–60 °C interval with 5 °C increments. It means that for Ch-W lower number of data points (5 instead of 9) were obtained, what resulted in smaller number of the degrees of freedom. As a result, the confidence intervals had extended. Although direct comparison between the results for asphaltene based sorbents and Ch-W is difficult, nevertheless it can be seen that the affinity (indicated by the value of ΔH_A) of probe molecules is stronger for the surface of Asf and Asf-Nitro sorbents, as compared to Ch-W, despite the three times higher temperature during experiments with asphaltene sorbents.

The forces responsible for the adsorption (intermolecular adsorbent-adsorbate interactions) can be generally divided into dispersive (γ_S^D) and specific (γ_S^{SP}) components of the surface free energy, corresponding to the dispersion and specific interactions, respectively. The dispersive component is unspecific for all molecules and is caused by London forces. In the Table 2 values of the γ_S^D for asphaltene sorbents are given along with the value comparing the difference (Asf-Nitro/Asf) that arise after chemical modification. The plot for the data in Table 2 can be found in Fig. S4.

Determination coefficient values for alkane reference lines were above 0.995 at almost all experimental temperatures. Obtained values of the γ_S^D indicate that asphaltene sorbents are very active and exhibit

Table 1
Values of enthalpies and entropies of adsorption. TCM – chloroform, THF – tetrahudrofuran, EtOAc – ethyl acetate, nBuOH – *n*-butanol. NA – not applicable; at the experimental conditions the retention was insufficient or excessive.

	Ch-W		Asf		Asf-Nitro	
T [K]	313–333		423–473		423–473	
Probe	ΔH_A (kJ/mol)	ΔS_A (J/mol)	ΔH_A (kJ/mol)	ΔS_A (J/mol)	ΔH_A (kJ/mol)	ΔS_A (J/mol)
C5	NA	NA	NA	NA	−52.06 ± 8.44	−98 ± 19
C6	−34.12 ± 8.34	−112 ± 26	−43.89 ± 8.13	−90 ± 18	−71.82 ± 17.60	−133 ± 39
C7	−59.83 ± 18.62	−182 ± 58	−59.24 ± 4.89	−119 ± 11	−94.28 ± 8.09	−173 ± 18
C8	−70.05 ± 22.83	−203 ± 71	−69.47 ± 2.70	−136 ± 6	−111.91 ± 8.21	−202 ± 18
C9	−77.76 ± 9.30	−217 ± 29	−80.36 ± 3.39	−155 ± 8	−124.81 ± 12.32	−220 ± 27
C10	−93.77 ± 14.59	−259 ± 45	−88.15 ± 4.21	−167 ± 9	NA	NA
TCM	−33.92 ± 7.30	−112 ± 23	−50.40 ± 9.38	−101 ± 21	−66.48 ± 5.32	−117 ± 12
THF	−43.11 ± 2.76	−113 ± 9	−54.12 ± 2.33	−106 ± 5	−81.70 ± 6.40	−144 ± 14
EtOAc	−53.09 ± 10.99	−144 ± 34	−61.54 ± 5.27	−123 ± 12	−97.74 ± 8.81	−174 ± 20
nBuOH	−44.04 ± 9.53	−109 ± 30	−55.32 ± 3.50	−101 ± 8	−100.97 ± 6.78	−175 ± 15
acetone	−38.70 ± 5.59	−102 ± 17	−48.96 ± 5.88	−96 ± 13	−83.18 ± 4.76	−148 ± 11
benzene	−34.01 ± 8.03	−110 ± 25	−51.49 ± 2.43	−100 ± 5	−76.64 ± 5.06	−133 ± 11

Table 2
Values of the dispersive component of the surface free energy for the Asf and Asf-Nitro adsorbents.

T [K]	γ_S^D (mJ m^{-2})				Asf-Nitro/Asf
	Asf	R^2	Asf-Nitro	R^2	
423	57.72 ± 0.01	1.000	197.50 ± 1.12	0.997	3.42 ± 0.02
428	55.32 ± 0.00	1.000	186.04 ± 0.69	0.998	3.36 ± 0.01
433	52.00 ± 0.03	1.000	175.64 ± 0.06	1.000	3.38 ± 0.00
438	49.79 ± 0.02	1.000	165.35 ± 0.29	0.999	3.32 ± 0.01
443	48.14 ± 0.06	0.999	146.80 ± 0.52	0.998	3.05 ± 0.01
448	44.17 ± 0.06	0.999	159.30 ± 0.42	0.998	3.36 ± 0.01
453	42.68 ± 0.04	0.999	155.87 ± 1.67	0.993	3.65 ± 0.04
458	36.07 ± 0.28	0.995	144.50 ± 1.13	0.995	4.01 ± 0.06
463	37.39 ± 0.09	0.998	130.24 ± 1.03	0.995	3.48 ± 0.04
468	37.58 ± 0.03	0.999	118.85 ± 0.74	0.996	3.16 ± 0.02
473	40.97 ± 0.33	0.999	113.09 ± 0.41	0.997	2.76 ± 0.03

strong dispersive interaction, as compared to Ch-W ($64.90 \pm 0.16\,\mathrm{mJ\,m^{-2}}$ at 313 K) despite that measurements for asphaltene sorbents were carried out at temperatures 3–4 times higher. It is clearly visible that the nitration promoted the dispersive interactions Asf-Nitro adsorbent have γ_S^D values 2.7–4 times higher than Asf adsorbent. The difference is the most substantial at lower temperatures and is diminishing as the experimental temperature increases. The increase in the γ_S^D value for the Asf-Nitro can be connected with the shortening of the side chains (see the FTIR analysis results), which can lower the steric hindrance and increase the access of the adsorbate molecules to the cores of the asphaltenes, which consists mostly of poly-condensed aromatic rings.

Values of the γ_S^D obtained for Asf-Nitro adsorbent are similar to those obtained for zeolite 13X and higher than those for alumina. Compared to values of γ_S^D found in the literature for activated carbon, Asf-Nitro exhibits slightly weaker dispersive interactions [64].

Analysis of theγ_S^D values obtained for tested sorbents at different temperatures revealed a temporary increase of the γ_S^D value at around 448 K. It could be explained with changes in the adsorption mechanism. As at the elevated temperatures the asphaltenes could swell and partial absorption phenomena could occur. In the previous GC studies an increased efficiency (narrower peaks) were observed for compounds eluting at higher temperatures during analyses with temperature programming, what is characteristic for gas-liquid chromatography. However similar trend should be observed for Asf adsorbent and while there are fluctuations of the γ_S^D value at around 448 K, but they are not statistically significant. Another possible explanation is that the mentioned increase in the dispersive interactions can be attributed to the surface modification and relaxation/deactivation of some surface groups leading to stronger interaction with the aromatic rings present in the core of the asphaltene structure.

For all adsorbents the value of γ_S^D is gradually decreasing with the temperature. The decrease in the γ_S^D value is the most evident for the Asf-Nitro. It is lowering at a rate of about $-3.0\,\mathrm{mJ\,m^{-2}\,K^{-1}}$ up to 448 K and $-1.9\,\mathrm{mJ\,m^{-2}\,K^{-1}}$ above 448 K, while for Asf and Ch-W adsorbents it is about -0.5 and $-1.0\,\mathrm{mJ\,m^{-2}\,K^{-1}}$, respectively. While this is tangential for adsorption step, during desorption it can be advantageous. 2–3 times higher decrease rate of dispersive interactions with increased temperature for Asf-Nitro, compared to Asf, means increased performance during regeneration process and higher economic feasibility.

Table S2 presents values of specific free energy change (ΔG_A^{SP}) for different polar molecules adsorbed on the investigated adsorbents at different temperatures. Both asphaltene adsorbents demonstrate fairly stable specific interactions in the range of experimental temperatures. Relative standard deviation (RSD%) of ΔG_A^{SP} for probe compounds is at the level of 10–15%. Examining changes of the ΔG_A^{SP} value for Asf-Nitro a sudden drop can be observed at around 458 K, which can be caused by lowering of the interactions provided by functional groups.

It is observed that values of specific interactions with basic compounds (THF and EtOAc) are largely higher for the Asf-Nitro, as compared to the Asf. That indicates increased acidity of the Asf-Nitro surface and is an expected result of nitration, as nitro groups should enhance acidic properties of a solid's surface. Contrary, there is no noticeable change in the value of ΔG_A^{SP} for TCM (acidic probe) between asphaltene adsorbents. Values of ΔG_A^{SP} for TCM and EtOAc reveals an amphoteric character of the Asf adsorbent, whereas Asf-Nitro surface displays enhanced acidic properties. In case of neutral compounds i.e. *n*-BuOH, acetone and benzene, only acetone exhibit significant change in the strength of specific interactions (caused by interactions of carbonyl group of acetone with nitro group of modified asphaltene). Thus, the considerable change (decrease) in the enthalpy of adsorption (see Table 1) for nBuOH and benzene is mainly a result of increased dispersive interactions, which is in line with measured γ_S^D values.

While strong specific interactions would be beneficial for removal of variety of compounds with different acceptor and donor-properties, extensive electron-acceptor character of Asf-Nitro surface will promote an adsorption of alkaline gases e.g. ammonia, pyridines or amines.

In Fig. 2, values of γ_S^+ to γ_S^- ratio for examined asphaltene adsorbents are presented. Exact values of the γ_S^+ and γ_S^- can be found in Table S3. Presented values are consistent with former discussion about ΔG_A^{SP} values. Asf exhibit a predominance of basic (electron-donor) properties over acidic, due to the presence of free electron pairs. Acid-base properties of the Asf surface are virtually stable over the range of experimental temperatures. The lower the γ_S^+ to γ_S^- ratio, the greater basicity of the solid's surface. It is evident that nitration shifted the character of the asphaltene's surface from basic to acidic. Electron-acceptor properties of Asf-Nitro are over 3 times stronger than electron-donor at 423 K and decrease with temperature increase. At 460 K acidity and basicity of Asf-Nitro surface is similar. Above that temperature, an increase of acidity is observed.

Values of the total surface energy (γ_S), divided into dispersive (γ_S^D) and specific (γ_S^{SP}) components, are shown in Fig. 3. It visualizes the aforementioned substantial increase in dispersive component of the free surface energy. According to values of γ_S, Asf-Nitro adsorbent exhibits significantly higher surface activity than unmodified adsorbent, being 3–4 times higher. For both examined asphaltene adsorbents, dispersive interactions dominate over specific interactions. Closer exami-

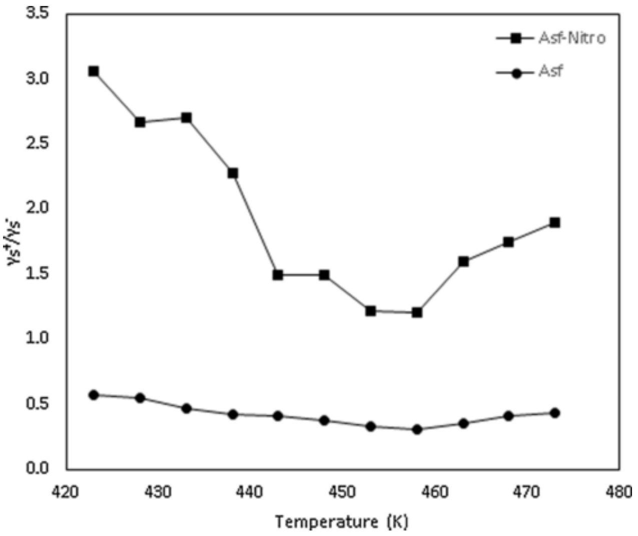

Fig. 2. Values of acidic to basic parameter ratios of examined asphaltene adsorbents.

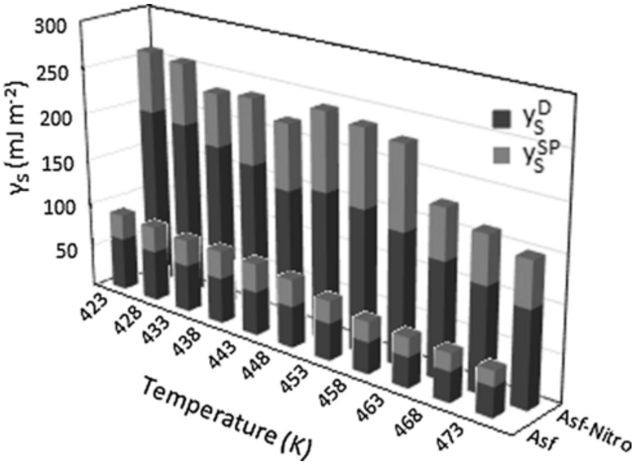

Fig. 3. Total surface energy of asphaltene adsorbents divided into dispersive and specific components.

nation of results revealed the increased contribution of specific components to the total surface energy. Taking into account that the surface energy has an immense impact on the adsorbent-adsorbate interactions, nitration appears as a favorable and uncomplicated modification that improve adsorption properties of asphaltenes and will increase the performance of asphaltene based sorbents.

To evaluate the impact of modification on asphaltene adsorbents capacity, measurements at finite concentration were carried out. Adsorption isotherms for TCM, n-BuOH and benzene were determined and fitted to the BET isotherm model. The results are presented in the Table 3. The monolayer adsorption capacity of the Asf-Nitro as a consequence of nitration was more than doubled. Increased q_{mono} values for benzene and nBuOH can be easily explained by increased dispersive interactions and in the case of BuOH by enhanced specific interactions as well.

What is intriguing is the Asf-Nitro's outstanding adsorption capacity for TCM (chloroform). TCM acts as an acid and it is expected to establish repulsive forces with the acidic surface of the Asf-Nitro. It may be explained by the predominance of the dispersive interactions and presence of basic adsorption centers. Although in the minority, they can diminish the repulsive effect of acidic moieties. Third factor can be the geometry of the molecules. TCM is not linear as n-BuOH or flat as benzene molecules and can be more "tightly" packed in the monolayer, even if cross-sectional areas of molecules are fairly similar.

Table 3
BET constant C, monolayer capacity q_{mono} and surface area of asphaltene adsorbent occupied by the adsorbate at 423–473 K. NA – retention was insufficient at experimental conditions to collect at least 5 data points.

Adsorbate	T (K)	q_{mono} (mg g^{-1})	C	R^2	SA (m^2 g^{-1})
	Asf				
Benzene	423	2.301 ± 0.522	110 ± 39	0.996	0.82 ± 0.19
	448	1.137 ± 0.185	165 ± 41	0.998	0.40 ± 0.07
	473	NA	NA	NA	NA
nBuOH	423	3.404 ± 0.738	51 ± 17	0.997	1.08 ± 0.23
	448	2.555 ± 0.709	66 ± 27	0.998	0.81 ± 0.23
	473	NA	NA	NA	NA
TCM	423	2.333 ± 0.312	215 ± 53	0.996	0.81 ± 0.09
	448	1.531 ± 0.483	355 ± 160	0.998	0.58 ± 0.22
	473	NA	NA	NA	NA
	Asf-Nitro				
Benzene	423	6.275 ± 0.795	804 ± 210	0.994	2.23 ± 0.28
	448	5.717 ± 0.664	569 ± 141	0.997	2.03 ± 0.24
	473	4.637 ± 0.655	479 ± 115	0.999	1.64 ± 0.23
nBuOH	423	7.647 ± 1.002	796 ± 357	0.993	2.43 ± 0.32
	448	6.574 ± 0.850	628 ± 225	0.994	2.09 ± 0.27
	473	4.636 ± 0.409	678 ± 147	0.998	1.47 ± 0.13
TCM	423	9.155 ± 1.198	891 ± 215	0.998	3.11 ± 0.41
	448	8.406 ± 0.683	656 ± 100	0.999	2.85 ± 0.23
	473	4.091 ± 1.778	1223 ± 352	0.985	1.39 ± 0.60

To give a more detailed description about the augmented adsorption properties of asphaltene sorbents, the surface area occupied by the adsorbate was calculated. The first thing that stands out is the similarity of the calculated SA for Asf adsorbent, to those provided by the manufacturer for N_2 adsorption (0.5–1.5 m^2 g^{-1}). The change in the SA values between asphaltene adsorbents is just the derivative of the aforementioned increased monolayer capacity and can be an indication of an introduction of a new adsorption sites to the surface.

4. Conclusion

The research revealed that a facile chemical modification can greatly increase the adsorption properties of asphaltene fraction. The nitrated adsorbent exhibits high surface activity that arise from enhanced dispersive and specific interactions. Compared to unmodified asphaltenes, a shift in Lewis acid-base properties after nitration was observed – from basic to acidic character of the surface. Moreover, in terms of dispersive interactions, nitrated sorbent is comparable with activated carbons, zeolites or alumina. Improved strength of the dispersive and specific interactions of nitrated asphaltenes lead to higher adsorption capacity for volatile organic compounds, as compared to unmodified sorbent.

Furthermore, wasted adsorbent can be regenerated at lower temperatures comparing to activated carbon. An alternative solution can be its incorporation into road bitumen – the asphaltene content in the bitumen is desired due to its valuable properties regarding improvement of basic bitumen applicational parameters such as penetration value or softening point.

Considering the above-mentioned assets of nitrated asphaltenes and the nature of the raw material (undesired by-product, facile isolation and modification method), nitrated asphaltenes appears to be an highly effective and low-cost adsorbent for gas phase removal of volatile organic compounds. Utilization of asphaltenes in separation processes would solve, at least partially, petroleum industry's problem with undesired and problematic by-product by its valorization. Moreover, asphaltene fraction's applications could be probably extended to liquid phase adsorption and other separation techniques e.g. membranes. Future studies should target the exploration of inexpensive porous supports for the asphaltene fraction that would facilitate the adsorption through the capillary condensation process as in case of activated carbons.

Acknowledgments

The authors gratefully acknowledge the financial support from the National Center for Research and Development, Warsaw, Poland – Project LIDER, no. LIDER/036/573/L-5/13/NCBR/2014. This work was financially supported by the project "INTERPHD2" no. POWR.03.02.00-IP.08-00-DOC/16.

Appendix A. Supplementary material

Supplementary data to this article can be found online at https://doi.org/10.1016/j.seppur.2019.05.041.

References

[1] J.H. Duffus, M. Nordberg, D.M. Templeton, Glossary of terms used in toxicology, Pure Appl. Chem. 79 (2007) https://doi.org/10.1351/pac200779071153.

[2] F.I. Khan, A.Kr. Ghoshal, A.K. Ghoshal, Removal of volatile organic compounds from polluted air, J. Loss Prev. Process Ind. 13 (2000) 527–545, https://doi.org/10.1016/S0950-4230(00)00007-3.

[3] I. Kourtchev, C. Giorio, A. Manninen, E. Wilson, B. Mahon, J. Aalto, M. Kajos, D. Venables, T. Ruuskanen, J. Levula, M. Loponen, S. Connors, N. Harris, D. Zhao, A. Kiendler-Scharr, T. Mentel, Y. Rudich, M. Hallquist, J.F. Doussin, W. Maenhaut, J. Bäck, T. Petäjä, J. Wenger, M. Kulmala, M. Kalberer, Enhanced volatile organic compounds emissions and organic aerosol mass increase the oligomer content of atmospheric aerosols, Sci. Rep. 6 (2016) https://doi.org/10.1038/srep35038.

[4] A. Mellouki, T.J. Wallington, J. Chen, Atmospheric chemistry of oxygenated volatile organic compounds: impacts on air quality and climate, Chem. Rev. 115 (2015) 3984–4014, https://doi.org/10.1021/cr500549n.

[5] L. Mølhave, B. Bach, O.F. Pedersen, Human reactions to low concentrations of volatile organic compounds, Environ. Int. 12 (1986) 167–175, https://doi.org/10.1016/0160-4120(86)90027-9.

[6] D.A. Sarigiannis, S.P. Karakitsios, A. Gotti, I.L. Liakos, A. Katsoyiannis, Exposure to major volatile organic compounds and carbonyls in European indoor environments and associated health risk, Environ. Int. 37 (2011) 743–765, https://doi.org/10.1016/J.ENVINT.2011.01.005.

[7] S.H. Hong, D.C. Shin, Y.J. Lee, S.H. Kim, Y.W. Lim, Health risk assessment of volatile organic compounds in urban areas, Hum. Ecol. Risk Assess. 23 (2017) 1454–1465, https://doi.org/10.1080/10807039.2017.1325714.

[8] R. Muñoz, E.C. Sivret, G. Parcsi, R. Lebrero, X. Wang, I.H. Suffet, R.M. Stuetz, Monitoring techniques for odour abatement assessment, Water Res. 44 (2010) 5129–5149, https://doi.org/10.1016/j.watres.2010.06.013.

[9] R. Iranpour, H.H.J. Cox, M.A. Deshusses, E.D. Schroeder, Literature review of air pollution control biofilters and biotrickling filters for odor and volatile organic compound removal, Environ. Prog. 24 (2005) 254–267, https://doi.org/10.1002/ep.10077.

[10] M. Nowicki, Planning of industrial sites in a city from the point of view of air pollution control, Energy Build. 11 (1988) 171–179, https://doi.org/10.1016/0378-7788(88)90034-5.

[11] P. Mudu, B. Terracini, M. Martuzzi (Eds.), Human Health in Areas with Industrial Contamination, WHO Regional Office for Europe, Copenhagen, 2014.

[12] European Parliament, European Council, Directive 2008/50/EC on ambient air quality and cleaner air for Europe, Off. J. Eur. Communities 152 (2008) 1–43.

[13] O. Penciu, M. Gavrilescu, Survey on the treatment of gaseous streams containing volatile organic compounds, Environ. Eng. Manag. J. 2 (2003).

[14] K.L. Foster, J. Economy, R.G. Fuerman, S.M. Larson, M.J. Rood, Adsorption characteristics of trace volatile organic compounds in gas streams onto activated carbon fibers, Chem. Mater. 4 (1992) 1068–1073, https://doi.org/10.1021/cm00023a026.

[15] W.J. Thomas, B. Crittenden, Adsorption Technology and Design, Elsevier, Oxford, 1998.

[16] X. Zhang, B. Gao, A.E. Creamer, C. Cao, Y. Li, Adsorption of VOCs onto engineered carbon materials: a review, J. Hazard. Mater. 338 (2017) 102–123, https://doi.org/10.1016/j.jhazmat.2017.05.013.

[17] J.-R. Li, R.J. Kuppler, H.-C. Zhou, Selective gas adsorption and separation in metal–organic frameworks, Chem. Soc. Rev. 38 (2009) 1477, https://doi.org/10.1039/b802426j.

[18] I.D. Manariotis, K.N. Fotopoulou, H.K. Karapanagioti, Preparation and characterization of biochar sorbents produced from malt spent rootlets, Ind. Eng. Chem. Res. 54 (2015) 9577–9584, https://doi.org/10.1021/acs.iecr.5b02698.

[19] Z. Chen, B. Chen, C.T. Chiou, Fast and slow rates of naphtalene sorption to biochars produced at different temperatures, Environ. Sci. Technol. 46 (2012) 11104–11111, https://doi.org/10.1021/es302345e.

[20] B.H. Hameed, A.A. Rahman, Removal of phenol from aqueous solutions by adsorption onto activated carbon prepared from biomass material, J. Hazard. Mater. 160 (2008) 576–581, https://doi.org/10.1016/J.JHAZMAT.2008.03.028.

[21] F.A.A. Al-Rub, M.H. El-Naas, I. Ashour, M. Al-Marzouqi, Biosorption of copper on Chlorella vulgaris from single, binary and ternary metal aqueous solutions, Process Biochem. 41 (2006) 457–464, https://doi.org/10.1016/j.procbio.2005.07.018.

[22] N. Maaloul, P. Oulego, M. Rendueles, A. Ghorbal, M. Díaz, Novel biosorbents from almond shells: characterization and adsorption properties modeling for Cu(II) ions from aqueous solutions, J. Environ. Chem. Eng. 5 (2017) 2944–2954, https://doi.org/10.1016/j.jece.2017.05.037.

[23] O.C. Mullins, The asphaltenes, Annu. Rev. Anal. Chem. 4 (2011) 393–418, https://doi.org/10.1146/annurev-anchem-061010-113849.

[24] L.A. Pineda, F. Trejo, J. Ancheyta, Correlation between properties of asphaltenes and precipitation conditions, Pet. Sci. Technol. 25 (2007) 105–119, https://doi.org/10.1080/10916460601054248.

[25] A.E. Pomerantz, Q. Wu, O.C. Mullins, R.N. Zare, Laser-based mass spectrometric assessment of asphaltene molecular weight, molecular architecture, and nanoaggregate number, Energy Fuels 29 (2015) 2833–2842, https://doi.org/10.1021/ef5020764.

[26] M.R. Gray, G. Assenheimer, L. Boddez, W.C. McCaffrey, Melting and fluid behavior of asphaltene films at 200–500 C, Energy Fuels 18 (2004) 1419–1423, https://doi.org/10.1021/ef049923w.

[27] C. Leyva, J. Ancheyta, C. Berrueco, M. Millán, Chemical characterization of asphaltenes from various crude oils, Fuel Process. Technol. 106 (2013) 734–738, https://doi.org/10.1016/j.fuproc.2012.10.009.

[28] B. Schuler, G. Meyer, D. Peña, O.C. Mullins, L. Gross, Unraveling the molecular structures of asphaltenes by atomic force microscopy, J. Am. Chem. Soc. 137 (2015) 9870–9876, https://doi.org/10.1021/jacs.5b04056.

[29] J. Murgich, Intermolecular forces in aggregates of asphaltenes and resins, Pet. Sci. Technol. 20 (2002) 983–997, https://doi.org/10.1081/LFT-120003692.

[30] K. Akbarzadeh, A. Hammami, A. Kharrat, D. Zhang, S. Allenson, J. Creek, S. Kabir, A. Jamaluddin, A.G. Marshall, R.P. Rodgers, O.C. Mullins, T. Solbakken, Asphaltenes—problematic but rich in potential, Oilf. Rev. (2007) 22–43.

[31] E. Ramirez-Jaramillo, C. Lira-Galeana, O. Manero, Modeling asphaltene deposition in production pipelines, Energy Fuels 20 (2006) 1184–1196, https://doi.org/10.1021/ef050262s.

[32] G. Boczkaj, M. Momotko, D. Chruszczyk, A. Przyjazny, M. Kamiński, Novel stationary phases based on asphaltenes for gas chromatography, J. Sep. Sci. 39 (2016) 2527–2536, https://doi.org/10.1002/jssc.201600183.

[33] M. Plata-Gryl, C. Jungnickel, G. Boczkaj, An improved scalable method of isolating asphaltenes, J. Pet. Sci. Eng. 167 (2018) 608–614, https://doi.org/10.1016/j.petrol.2018.04.039.

[34] W. Shen, Z. Li, Y. Liu, Surface chemical functional groups modification of porous carbon, Recent Patents Chem. Eng. (2012) https://doi.org/10.2174/2211334710801010027.

[35] M.S. Shafeeyan, W.M.A.W. Daud, A. Houshmand, A. Arami-Niya, Ammonia modification of activated carbon to enhance carbon dioxide adsorption: effect of pre-oxidation, Appl. Surf. Sci. (2011) https://doi.org/10.1016/j.apsusc.2010.11.127.

[36] M.S. Shafeeyan, A. Houshmand, A. Arami-Niya, H. Razaghizadeh, W.M.A.W. Daud, Modification of activated carbon using nitration followed by reduction for carbon dioxide capture, Bull. Korean Chem. Soc. (2015) https://doi.org/10.1002/bkcs.10100.

[37] W.D. Samuels, N.H. LaFemina, V. Sukwarotwat, W. Yantasee, X.S. Li, G.E. Fryxell, Chloromethylated activated carbon: a useful new synthon for making a novel class of sorbents for heavy metal separations, Sep. Sci. Technol. (2010) https://doi.org/10.1080/01496390903423550.

[38] M. Abe, K. Kawashima, K. Kozawa, H. Sakai, K. Kaneko, Amination of activated carbon and adsorption characteristics of its aminated surface, Langmuir (2000) https://doi.org/10.1021/la990976t.

[39] H. Ikeda, Y. Takeuchi, H. Asaba, Removal of H_2S, CH_3SH and $(CH_3)_3N$ from air by use of chemically treated activated carbon, J. Chem. Eng. Jpn. (1988) https://doi.org/10.1252/jcej.21.91.

[40] J. Schultz, L. Lavielle, C. Martin, The role of the interface in carbon-fiber epoxy composites, J. Adhes. 23 (1987) 45–60.

[41] E. Papirer, J. Schultz, C. Turchi, Surface properties of a calcium carbonate filler treated with stearic acid, Eur. Polym. J. 20 (1984) 1155–1158, https://doi.org/10.1016/0014-3057(84)90181-2.

[42] P.P. Ylä-Mäihäniemi, J.Y.Y. Heng, F. Thielmann, D.R. Williams, Inverse gas chromatographic method for measuring the dispersive surface energy distribution for particulates, Langmuir 24 (2008) 9551–9557, https://doi.org/10.1021/la801676n.

[43] F. Thielmann, Introduction into the characterisation of porous materials by inverse gas chromatography, J. Chromatogr. A 1037 (2004) 115–123, https://doi.org/10.1016/J.CHROMA.2004.03.060.

[44] A.T. James, A.J.P. Martin, Gas-liquid partition chromatography. A technique for the analysis of volatile materials, Analyst 77 (1952) 915–931, https://doi.org/10.1039/AN9527700915.

[45] A. Voelkel, B. Strzemiecka, K. Adamska, K. Milczewska, Inverse gas chromatography as a source of physiochemical data, J. Chromatogr. A. 1216 (2009) 1551–1566, https://doi.org/10.1016/J.CHROMA.2008.10.096.

[46] G.M. Dorris, D.G. Gray, Adsorption of n-alkanes at zero surface coverage on cellulose paper and wood fibers, J. Colloid Interface Sci. 77 (1980) 353–362, https://doi.org/10.1016/0021-9797(80)90304-5.

[47] C. Saint Flour, E. Papirer, Gas-solid chromatography. A method of measuring surface free energy characteristics of short glass fibers. 1. Through adsorption isotherms, Ind. Eng. Chem. Prod. Res. Dev. 21 (1982) 337–341, https://doi.org/10.1021/i300006a029.

[48] C. Saint Flour, E. Papirer, Gas-solid chromatography. A method of measuring surface free energy characteristics of short glass fibers. 2. Through retention volumes measure near zero surface coverage, Ind. Eng. Chem. Prod. Res. Dev. 21 (1982) 666–669, https://doi.org/10.1021/i300006a029.

[49] C.J. van Oss, R.J. Good, M.K. Chaudhury, Additive and nonadditive surface tension components and the interpretation of contact angles, Langmuir 4 (1988) 884–891, https://doi.org/10.1021/la00082a018.

[50] P.J. Kipping, D.G. Winter, Measurement of adsorption isotherms by a gas chromatographic technique, Nature 205 (1965) 1002–1003, https://doi.org/10.1038/2051002a0.

[51] J.F.K. Huber, R.G. Gerritse, Evaluation of dynamic gas chromatographic methods for the determination of adsorption and solution isotherms, J. Chromatogr. A 58 (1971) 137–158, https://doi.org/10.1016/S0021-9673(00)96607-X.

[52] R: A Language and Environment for Statistical Computing, 2008. http://www.r-project.org.

[53] T. V. Elzhov, K.M. Mullen, A.-N. Spiess, B. Bolker, minpack.lm: R Interface to the Levenberg-Marquardt nonlinear least-squares algorithm found in MINPACK, plus support for bounds, 2016.

[54] S. Akmaz, O. Iscan, M.A. Gurkaynak, M. Yasar, The structural characterization of saturate, aromatic, resin, and asphaltene Fractions of Batiraman crude oil, Pet. Sci. Technol. 29 (2011) 160–171, https://doi.org/10.1080/10916460903330361.

[55] O.C. Mullins, E.Y. Sheu, Structures and Dynamics of Asphaltenes, Plenum Press, New York, 1998.

[56] B.K. Wilt, W.T. Welch, J. Graham Rankin, Determination of asphaltenes in petroleum crude oils by Fourier transform infrared spectroscopy, Energy Fuels 12 (1998) 1008–1012, https://doi.org/10.1021/ef980078p.

[57] S.I. Andersen, Separation of asphaltenes by polarity using liquid-liquid extraction, Pet. Sci. Technol. 15 (1997) 185–198, https://doi.org/10.1080/10916469708949650.

[58] V.M. Malhotra, H.A. Buckmaster, 34 GHz EPR FTIR spectra of chromatographically separated Boscan asphaltene fractions, In: Prepr. from ACS Symp. Trace Elem. Pet. Geochemistry, Dallas, 1989, pp. 185–191.

[59] M.F. Ali, M.N. Siddiqui, A.A. Al-Hajji, Structural studies on residual fuel oil asphaltenes by RICO method, Pet. Sci. Technol. 22 (2004) 631–645, https://doi.org/10.1081/LFT-120034205.

[60] M.N. Siddiqui, I.W. Kazi, Chlorination, nitration, and amination reactions of asphaltene, Pet. Sci. Technol. 32 (2014) 2987–2994, https://doi.org/10.1080/10916466.2014.924528.

[61] J. Douda, Ma.E. Llanos, A.R. Alvarez, J.N. Bolaños, Structure of Maya asphaltene−resin complexes through the analysis of soxhlet extracted fractions, Energy Fuels 18 (2004) 736–742, https://doi.org/10.1021/EF034057T.

[62] L.M. Petrova, N.A. Abbakumova, T.R. Foss, G.V. Romanov, Structural features of asphaltene and petroleum resin fractions, Pet. Chem. 51 (2011) 252–256, https://doi.org/10.1134/S0965544111040062.

[63] H.H. Ibrahim, R.O. Idem, Correlations of characteristics of Saskatchewan crude oils/asphaltenes with their asphaltenes precipitation behavior and inhibition mechanisms: differences between CO_2- and n-heptane-induced asphaltene precipitation, Energy Fuels 18 (2004) 1354–1369, https://doi.org/10.1021/ef034044f.

[64] E. Díaz, S. Ordóñez, A. Vega, J. Coca, Adsorption characterisation of different volatile organic compounds over alumina, zeolites and activated carbon using inverse gas chromatography, J. Chromatogr. A 1049 (2004) 139–146, https://doi.org/10.1016/j.chroma.2004.07.061.